Characteristic determinant approach to the spectrum of one-dimensional $\mathcal{PT}$-symmetric systems

Vladimir Gasparian [1,*] Peng Guo [2,3,†] Antonio Pérez-Garrido [4,‡] and Esther Jódar [4,§]
[1]Department of Physics and Engineering, California State University, Bakersfield, California 93311, USA
[2]College of Arts and Sciences, Dakota State University, Madison, South Dakota 57042, USA
[3]Kavli Institute for Theoretical Physics, University of California, Santa Barbara, California 93106, USA
[4]Departamento de Física Aplicada, Universidad Politécnica de Cartagena, E-30202 Murcia, Spain

(Received 26 March 2025; accepted 29 August 2025; published 15 September 2025)

We obtain a closed-form expression for the energy spectrum of $\mathcal{PT}$-symmetric superlattice systems with complex potentials of periodic sets of two δ potentials in the elementary cell. In the presence of periodic gain and loss, we analyzed in detail a diatomic crystal model, varying either the scatterer distances or the potential heights. It is shown that at a certain critical value of the imaginary part of the complex amplitude, topological states depending on the lattice size and the configuration of the unit cell can be pushed out from the given region. This may happen at the $\mathcal{PT}$-symmetry breaking (exceptional) points.

DOI: 10.1103/d9wj-v62g

I. INTRODUCTION

It is known that when the energy momentum dispersion relation is invariant under the joint action of parity ($x \to -x$) and time reversal ($i \to -i$) (see, e.g., Refs. [1,2] and references therein), the eigenvalues of the Hamiltonian are real (so-called $\mathcal{PT}$-symmetric system), in spite of the fact that the potential is complex. Such $\mathcal{PT}$-symmetric complex potentials must satisfy the condition $V^*(-x) = V(x)$ and their contact with the environment is highly constrained so that gain from the environment and loss to the environment are exactly balanced. For optical systems with $\mathcal{PT}$-symmetric properties, the potential $V(x)$ in the Schrödinger equation is replaced by the refractive index profile $\epsilon^*(-x) = \epsilon(x)$ in the Helmholtz equation. The systems with alternating gain and loss regions demonstrate many novel optical properties (for recent reviews, see Refs. [1,3]). The interplay between gain and index modulation has emerged as a fruitful research area in photonics. The $\mathcal{PT}$ symmetry, found with experimental realizations in the field of photonics in artificial materials with spatial distributions of real and complex permittivities, shows the ability of molding the flow of light (see Refs. [4–6]).

Most articles devoted to $\mathcal{PT}$-symmetric systems are related to the study of the problems of eigenvalues and their characteristics [4–8] (e.g., the number of eigenvalues, reality, exceptional points for which the eigenstates in the general case are not mutually orthogonal, etc.). Recently, the effort has been extended to scattering problems (see, e.g., Refs. [9–14] and references therein), and even less to the tunneling time problem [15–17] and Faraday/Kerr effect [18,19].

The aim of this paper is to carry out a generalization of the method of characteristic determinant, developed for the real and complex potentials in Refs. [19,20], to the spectrum of $\mathcal{PT}$-symmetric superlattice systems with complex potentials of periodic sets of δ potentials with n centers in the elementary cell [see Eq. (16)].

The characteristic determinant method is compatible with the transfer matrix method and allows in some cases to carry out efficient analytical calculations when the number of scattering potentials become very large, in contrast to the transfer matrix method, which in such cases becomes practically useless. It, based on conventional scattering formalism, depends on the amplitudes of reflection of a single scatterer only and does not require further tight-binding approximations. The key idea is to start from a single cell and gradually build up to a many-cell system by adding one cell at a time mapping the problem of the calculation of the determinant D_N of order $N \times N$ (N is the number of individual scattering sites or atoms in a chain). Note that the local and average density of states for the sample, the reciprocal of the transmission amplitude, and the characteristic tunneling time of the barrier [21,22] are directly related to the determinant D_N.

The model of $\mathcal{PT}$-symmetric systems of delta potentials, presented by Eq. (16), leads to an exact analytical expression for the energy spectrum of electrons in the infinite square well with arbitrary N Dirac delta function potentials depending on the values of the gain-loss parameters.

Particularly for a diatomic crystal ($n = 2$ atoms in a unit cell), varying either the scatterer distances or the potential heights, we obtained a closed-form expression for the energy spectrum in terms of the number of cells, the real and imaginary parts of the complex amplitudes of δ potentials, and separation of the potentials. It is shown that at a certain

*Contact author: vgasparyan@csub.edu
†Contact author: peng.guo@dsu.edu
‡Contact author: antonio.perez@upct.es
§Contact author: esther.jferrandez@upct.es

critical value of the imaginary part of the complex amplitude, the topological states may move from given regions. This may happen at the $\mathcal{PT}$-symmetry breaking (exceptional) points. Recently, the properties of the topologically protected edge states for the $\mathcal{PT}$-symmetric extension of the Su-Schrieffer-Heeger model governed by the non-Hermitian Hamiltonian were studied both numerically and analytically in Ref. [23]. A topologically nontrivial non-Hermitian trimerized optical lattice is investigated in Ref. [24].

The work is organized as follows. In Sec. II, we formulated the problem of determining the energy spectrum through the characteristic determinant. In Sec. III, we consider the technically simple case of the periodic structure with two delta potentials in a unit cell. For these finite bipartite Kroning-Penney $\mathcal{PT}$-symmetric models, appropriate analytical expressions for scattering matrix elements and for gain/loss parameters are derived. The main conclusions are summarized in Sec. IV.

II. ENERGY SPECTRUM IN TERMS OF THE CHARACTERISTIC DETERMINANT: GENERAL STATEMENT

A. Short summary of the characteristic determinant method for open systems

It is known that the poles of Green's functions (GFs) in open systems correspond to the spectrum of excitations; meanwhile in the case of a closed system, the poles coincide with energy spectrum of the system. However, calculating the GF for any system with an arbitrary potential $V(x)$ is a difficult task. Technically, the problem is that the calculation of the GF, which can always be written in the form of a bilinear expansion in eigenfunctions, requires knowledge of the latter, i.e., an exact solution of the Schrödinger equation. That is why, explicit expressions for GF are known only for a few specific potentials (see, e.g., Refs. [25,26] and references therein). Surprisingly, it often turns out that calculating the poles (or zeros of the characteristic determinant) of the GF is, from a technical point of view, relatively simpler than calculating the GF itself. For the Kronig-Penney and tight-binding models, the poles have been calculated in quasi-one- and two-dimensional disordered systems without any limitation on the number of impurities and modes in terms of the so-called characteristic determinants in Refs. [19,20]. This nonperturbative approach sufficiently describes electron (photon) behavior in a random potential and allows one to study the energy spectrum and scattering matrix elements in any system without actually determining the electron (photon) eigenfunctions. Once characteristic determinant D_N is obtained, the determination of the bound states is easy. It can be shown [19,20,25,27] that the poles of the GF of the whole system (which, as we know, correspond to the bound states) are just the zeros of the characteristic determinant. Therefore, to find the bound states of the potential for both models, we just will have to solve the equation $D_N = 0$. The determinant D_N is in general a complex function of the energy E. Hence, we need to find simultaneous zeros in its real and imaginary parts.

In what follows, we will present some details of characteristic determinant method. Based on Refs. [19,20], the characteristic determinant D_N of a one-dimensional chain of N δ potential with complex amplitudes $Z_l \equiv \eta_{1l} + i\eta_{2l}$ and corresponding coordinates x_l is defined by

$$D_N = \det\left(M_{n,l}^{(N)}\right), \tag{1}$$

where

$$M_{n,l}^{(N)} = \delta_{n,l} + \frac{iZ_l}{2k} e^{ik|x_l - x_n|}, \quad 1 \leqslant (n,l) \leqslant N. \tag{2}$$

k denotes the momentum of electron. The total energy of an electron E is related to momentum k by $E = k^2$, where the mass of electron is assumed as $1/2$ in this work. The characteristic determinant D_N can also be written as the determinant of a tridiagonal Toeplitz matrix and satisfies the following recurrence relationship:

$$D_N = A_N D_{N-1} - B_N D_{N-2}, \tag{3}$$

where D_{N-1} (D_{N-2}) is the determinant [Eq. (2)] with the Nth [and also the $(N-1)$th] row and column omitted. The coefficients A_N and B_N can be obtained from the explicit form of $M_{n,l}^{(N)}$. For $N > 1$, we have

$$A_N = 1 + B_N + \frac{iZ_N}{2k}\left(1 - e^{2ik(x_N - x_{N-1})}\right) \tag{4}$$

and

$$B_N = \frac{iZ_N}{Z_{N-1}} e^{2ik(x_N - x_{N-1})}. \tag{5}$$

The initial conditions for the recurrence relations are

$$D_0 = 1, \quad D_{-1} = 0, \quad A_1 = 1 + \frac{iZ_1}{2k}, \quad B_1 = 0. \tag{6}$$

The transmission amplitude t is the inverse of the characteristic determinant D_N multiplied by the phase accumulated during the transmission, i.e.,

$$t = e^{ik(x_N - x_1)} D_N^{-1}, \tag{7}$$

while the left and right propagating reflection amplitudes r_L and r_R are given by

$$r_L = -\frac{2k}{iZ_1}\frac{D_N - D_{-1+N}}{D_N} - 1 \equiv i\frac{\partial \ln t}{\partial \frac{Z_1}{2k}} - 1 \tag{8}$$

and

$$r_R = -\frac{2k}{iZ_N}\frac{D_N - D_{N-1}}{D_N} - 1 \equiv i\frac{\partial \ln t}{\partial \frac{Z_N}{2k}} - 1, \tag{9}$$

respectively. Here, D_{-1+N} is the characteristic determinant without the first delta function (i.e., $Z_1 = 0$), and D_{N-1} is the characteristic determinant without the last delta function (i.e., $Z_N = 0$).

B. Quantization condition of closed systems with hard wall boundary conditions

In order to further investigate the energy spectrum of the closed system with hard wall boundary conditions, let us, following Ref. [28], write explicitly the dependence of the characteristic determinant D_N on Z_1 and Z_N for our general system of multiple δ potentials. From the recurrence relations

for the characteristic determinant [Eq. (3)] applied to both ends, we can rewrite D_N in the following way ($m \equiv N-2$):

$$D_N(Z_1, Z_N) = D_m\left(1 + \frac{A_m}{2k} iZ_1 + \frac{B_m}{2k} iZ_N + \frac{C_m}{4k^2} Z_1 Z_N\right), \tag{10}$$

where D_m is the characteristic determinant for the previous potential without the first and the last delta function (i.e., $Z_1 = Z_N = 0$), and A_m, B_m, and C_m are coefficients independent of Z_1 and Z_N and involving D_m. These coefficients are defined as

$$A_m = 1 - i\sqrt{1-T_m}\, e^{i\Theta_1}, \tag{11}$$

$$B_m = 1 - i\sqrt{1-T_m}\, e^{i\Theta_2}, \tag{12}$$

and

$$C_m = 2ie^{i\frac{\Theta_1+\Theta_2}{2}}\left[\sin\left(\frac{\Theta_1+\Theta_2}{2}\right) + \sqrt{1-T_m}\cos\left(\frac{\Theta_1-\Theta_2}{2}\right)\right], \tag{13}$$

where $T_m = t_m t_m^*$ is the transmission coefficient of the system of m contact potentials. The transmission amplitude through the system, t_m, is determined by Eq. (7) with D_N replaced by D_m, and $(x_N - x_1)$ replaced by $(x_{N-1} - x_2)$. The phases appearing in the previous equations are defined as

$$\Theta_1 = \varphi_m + \varphi_{a,m} + 2k(x_2 - x_1),$$
$$\Theta_2 = \varphi_m - \varphi_{a,m} + 2k(x_N - x_{N-1}), \tag{14}$$

where φ_m is the phase accumulated in a transmission event and $\varphi_{a,m}$ is the phase characterizing the asymmetry between the reflection to the left and to the right of the block with m contact potentials.

Note that the expression in Eq. (10) for $D_N(Z_1, Z_N)$ is written for an open system. To close the system with hard wall boundary conditions on both ends of chain and obtain the desired expression for the energy spectrum, it is necessary to increase the amplitudes of the delta potentials Z_1 and Z_N. In the limit of Z_1 and Z_N tending to infinity, we keep only the leading term $C_m \frac{Z_1 Z_N}{4k^2}$ in $D_N(Z_1, Z_N)$. The zeros of the C_m yield the quantization condition that determines the energy spectrum of systems confined by hard wall boundary conditions; hence, a compact expression of quantization condition can be obtained:

$$\sin(\varphi_m + k(x_N - x_{N-1} - x_1 + x_2)) + \sqrt{1-T_m}\cos(\varphi_{a,m} - k(x_N - x_{N-1} - x_2 + x_1)) = 0, \tag{15}$$

where x_N and x_1 are the ends of the chain where the hard walls are located, and x_2 and x_{N-1} are the first and last coordinates of the block with m contact delta potentials.

We remark that though we arrived at the above equation using the δ-potential model, it can be generalized to an arbitrarily shaped potential by following Ref. [29]. Therefore, Eq. (15) is a fairly general expression regardless of the shape of the potential under consideration. It can be used to find the energy spectrum of electrons in any finite closed one-dimensional (1D) system divided into three blocks (see Sec. III).

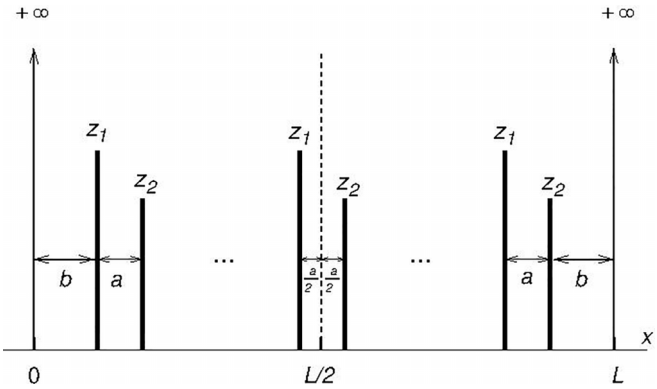

FIG. 1. Demo plot of a $\mathcal{PT}$-symmetric system with two δ potentials in a unit cell, described by Eq. (16).

III. FINITE BIPARTITE KRONING-PENNEY $\mathcal{PT}$-SYMMETRIC MODEL

In what follows, we analyze in detail the spectrum of 1D finite Kronig-Penney complex nonconservative model, by using quantization condition given in Eq. (15).

The mathematical model of the $\mathcal{PT}$-symmetric superlattice systems with complex potentials discussed below is the infinite well with $2M$ Dirac delta function potentials with complex strengths that are distributed in the following way:

$$V(x) = \sum_{n=1}^{M}[Z_1\delta(x - (nd - a)) + Z_2\delta(x - nd)], \tag{16}$$

where d is the lattice period and a is the distance between two successive potentials Z_1 and Z_2, $Z_1 = Z_2^* \equiv \eta_1 + i\eta_2$ (η_2 represents non-Hermitian degree). The system has M cells and $2M$ scatterers. The hard walls are placed at $x = 0$ and $x = L$, where $L = b + Md$ and $b = d - a$ (see Fig. 1), and the wave function vanishes when $x < 0$ and $x > L$. A closed system with $2M$ finite delta potentials located in between two infinite potentials is obtained. The $\mathcal{PT}$ symmetry requirement is equivalent to

$$V\left(x - \frac{L}{2}\right) = V^*\left(-x + \frac{L}{2}\right).$$

The transmission coefficient T_m through the system and the phase φ_m, accumulated during the transmission and the phase difference $\varphi_{a,m}$ between the reflection from the left and from the right, entering in the Eq. (15), can be evaluated by using the method of the characteristic determinant, developed in Refs. [19,20].

Before going into the details of the quantization condition given by Eq. (15), we present several useful relations characterizing the $\mathcal{PT}$-symmetric model.

After some algebraic manipulations, we find

$$T_m^{-1} \equiv |D_m|^2 = 1 + \sqrt{|D_2|^2 - 1}\frac{\sin^2(M\beta d)}{\sin^2(\beta d)}, \tag{17}$$

$$\varphi_m = -kb - \arctan\left[\frac{\mathrm{Im}[e^{-ikd}D_2]}{\mathrm{Re}[e^{-ikd}D_2]}\right], \tag{18}$$

and

$$\varphi_{a,m} = 2\arctan\left[\frac{\left(\frac{Z_2}{2k}-\frac{Z_1}{2k}\right)\sin(ka)}{\left(\frac{Z_2}{2k}+\frac{Z_1}{2k}\right)\cos(ka)+2\frac{Z_1}{2k}\frac{Z_2}{2k}\sin(ka)}\right], \tag{19}$$

where again $b = d - a$ is the distance between the left (right) hard wall and the first (last) delta potential: $x_{2M} - x_{2M-1} = x_2 - x_1 \equiv b$. The characteristic determinant D_2 of one cell with two delta potentials is defined by

$$D_2 = \det\begin{pmatrix} 1+i\frac{Z_1}{2k} & i\frac{Z_2}{2k}e^{ika} \\ i\frac{Z_1}{2k}e^{ika} & 1+i\frac{Z_2}{2k}\end{pmatrix}. \tag{20}$$

Taking into account the periodicity of the system and using recurrence relations in Eq. (2), one can also show that the important quantity D_m for a diatomic crystal may be written in the form [22]

$$D_m = e^{ikMd}\left\{\cos(M\beta d) + iIm[e^{-ikd}D_2]\frac{\sin(M\beta d)}{\sin(\beta d)}\right\}, \tag{21}$$

where β plays the role of quasimomentum for the diatomic crystal and is given by the equation

$$\cos(\beta d) \equiv \mathrm{Re}[e^{-ikd}D_2] = \cos(kd) + \left(\frac{Z_1}{2k}+\frac{Z_2}{2k}\right)\sin(kd) + 2\frac{Z_1}{2k}\frac{Z_2}{2k}\sin(ka)\sin k(d-a). \tag{22}$$

As for the term $\mathrm{Im}[e^{-ikd}D_2]$ in Eq. (21), it can be written in the form

$$\mathrm{Im}[e^{-ikd}D_2] \equiv \left(\frac{Z_1}{2k}+\frac{Z_2}{2k}\right)\cos(kd) - \sin(kd) + 2\frac{Z_1}{2k}\frac{Z_2}{2k}\sin(ka)\cos k(d-a). \tag{23}$$

Finally, after some algebraic manipulation, Eq. (15) yields a compact form of quantization condition:

$$\frac{\sin(kb)\sin((M+1)\beta d) + \sin(M\beta d)\sin(ka)}{\sin\beta d} = 0. \tag{24}$$

Equation (24) is our main general result for the energy spectrum of $\mathcal{PT}$-symmetric superlattice systems. It holds for both real and complex potentials, extending several well-known results in the literature, and helps to get even more insight into the mathematical structures of the eigenvalues. To demonstrate this explicitly, it is useful to consider the relatively simple finite bipartite Kroning-Penney model discussed, e.g., in Refs. [5,30–32] for real potentials. We want to emphasize here that one can use Eqs. (24) and (25) as a starting point in reproducing the most of the main results of Refs. [5,30–32], calculated numerically.

A. Real potentials

In case of a simple Kroning-Penney model, i.e., $Z_1 = Z_2 \equiv V_0 > 0$ (single positive delta potential in a cell: $d = 2a$ and $b = a$), the above expression, Eq. (24), reduced to

$$\sin(ka)\frac{\sin(m+1)\beta a}{\sin(\beta a)} = 0, \tag{25}$$

where now m is the number of delta potentials (even or odd) and $\cos(\beta a)$ is defined as

$$\cos(\beta a) = \cos(ka) + \frac{V_0}{2k}\sin(ka). \tag{26}$$

Note that for particular values of $m = 1$ and $m = 2$, the above formula reduces to the results found in Refs. [32,33], using a different approach. Note also that the expression in Eq. (25) is similar in spirit, but differs in the details of the physical context from some other known results where interference plays a critical role. The class of phenomena to which this applies is the light diffraction through multiple slits, Landauer's resistance between an ideal conductor and a periodic structure, traversal, dwell, and tunneling times of particles (photons or electrons) traveling through periodic systems, etc. For example, the zeros of the energy spectrum of the simple Kroning-Penney model with m delta potentials [Eq. (25)] formally coincide (in units of e^2/h) with the zeros of the two terminal Landauer's resistance between an ideal conductor and a periodic structure with $(m+1)$ delta potentials in Ref. [20]:

$$\rho_{m+1} = |D_{m+1}|^2 - 1 \equiv \frac{1-T_{m+1}}{T_{m+1}} = \left(\frac{V_0}{2k}\right)^2\frac{\sin^2(m+1)\beta a}{\sin^2(\beta a)}. \tag{27}$$

B. Complex $\mathcal{PT}$-symmetric potentials

After a brief discussion of the energy spectrum, given by Eq. (24), at real potentials, let us analyze the spectrum when $Z_1 = Z_2^* = \eta_1 + i\eta_2$ is an arbitrary complex number.

Similar to the above derivation of Eq. (24), one can show that the energy spectrum in case of an arbitrary complex number of Z formally is still given by the same equation. As for $\cos(\beta d)$, we write it explicitly in terms of η_1 and η_2:

$$\cos(\beta d) = \cos(kd) + \frac{\eta_1}{k}\sin(kd) + \frac{\eta_1^2+\eta_2^2}{2k^2}\sin(ka)\sin(kb). \tag{28}$$

We now analyze the energy spectrum expression (24) for different η_1 and η_2, based on relation in Eq. (28), to see a dynamical evolution of the band structure depending on the imaginary portion η_2 (see, e.g., Figs. 2 and 3). Figures 2(c) and 3(c) show the band structure for a chain consisting of $M = 10$ cells or 20 positive δ-like potentials as a function of a with fixed $d = 1$ and $\eta_2 = 0$. The parameter a can be considered as a shift relative to the wall of the box and ultimately play the role of some additional virtual second dimension in studying the topology of the bands (see, e.g., Ref. [34]. A similar situation with an additional degree of freedom, which is typical of the topic of topological insulator in one-dimensional system, arises in the case of a tight-binding model with a modulated tunneling parameter [35]. As seen from Figs. 2(c) and 3(c), there are states that are separating from the upper band and move to lower band through the forbidden gap. For example, the extra level on the right-hand side in Fig. 3(c) between the first and the second bands is the signature of topological edge states; see, e.g., the discussion of a bipartite Kronig-Penney model in Ref. [30], which would be absent if the hard wall boundary is replaced by an infinite long periodic system.

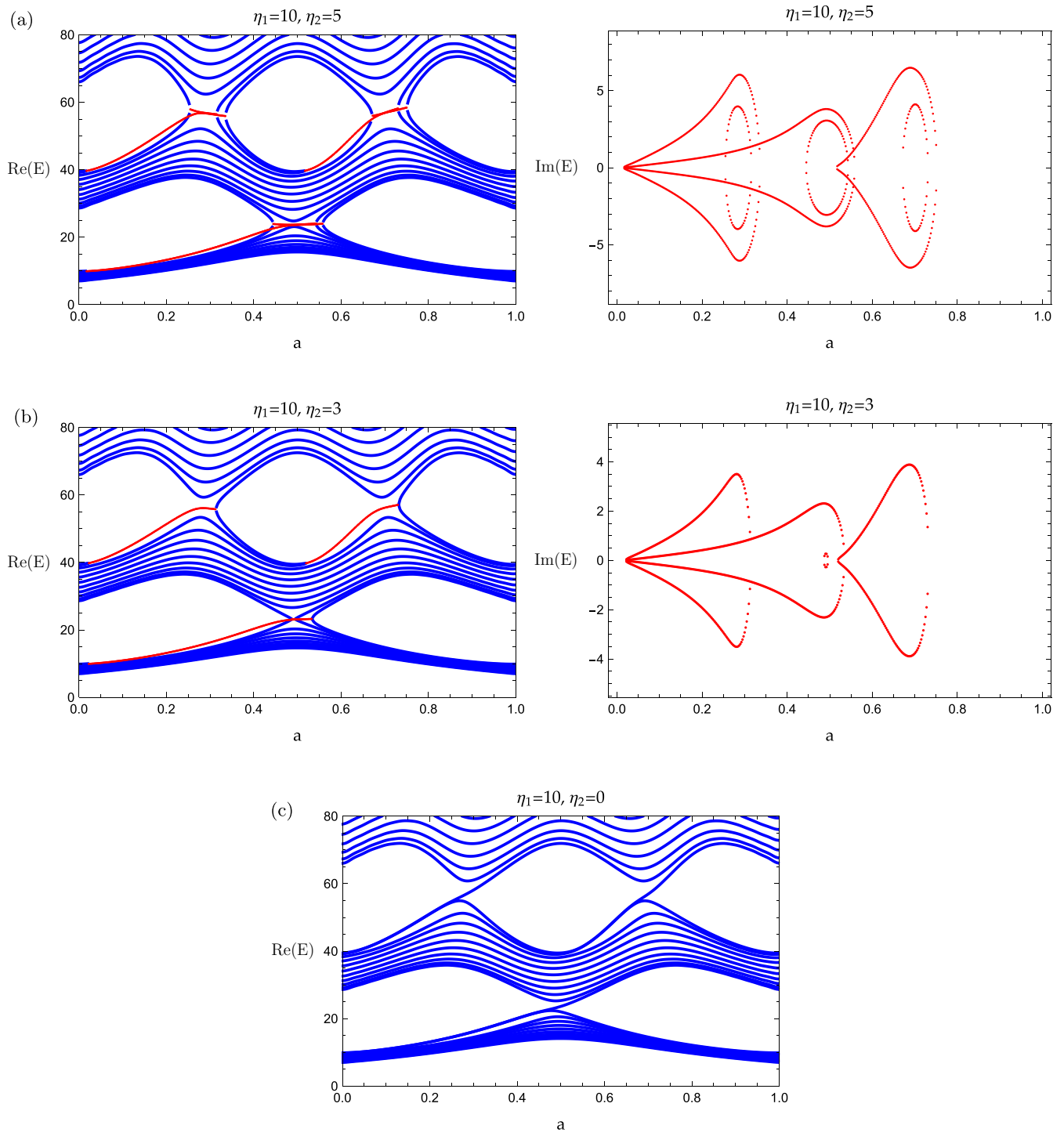

FIG. 2. The real and imaginary parts of energy spectrum as a function of the distance $a = 1 - b$ between two δ potentials z_1 and z_1^* for $\eta_1 = +10$ positive strength and varying η_2. The real energy solutions are plotted in blue, and the complex energy solutions are plotted in red. The number of cells is $M = 10$. (a) Real (left) and imaginary (right) parts of eigen-energy with $\eta_1 = 10$ and $\eta_2 = 5$. (b) Real (left) and imaginary (right) parts of eigen-energy with $\eta_1 = 10$ and $\eta_2 = 3$. (c) Real eigen-energy with $\eta_1 = 10$ and $\eta_2 = 0$.

These extra topological edge levels are also demonstrated in Fig. 3(a) with hard wall boundary condition compared with Fig. 5 for a periodic infinite long system where topological edge states are absent. In principle, the Zak phase and the winding number of the reflection coefficient could be evaluated for topological states (see, e.g., Ref. [30]. The surface, interface, or contact states that arise at the boundary of two systems in common gap can be exponentially localized to the edges. They are determined by the poles of the reflection amplitudes, left, r_L in Eq. (8), or right, r_R in Eq. (9). Positions of

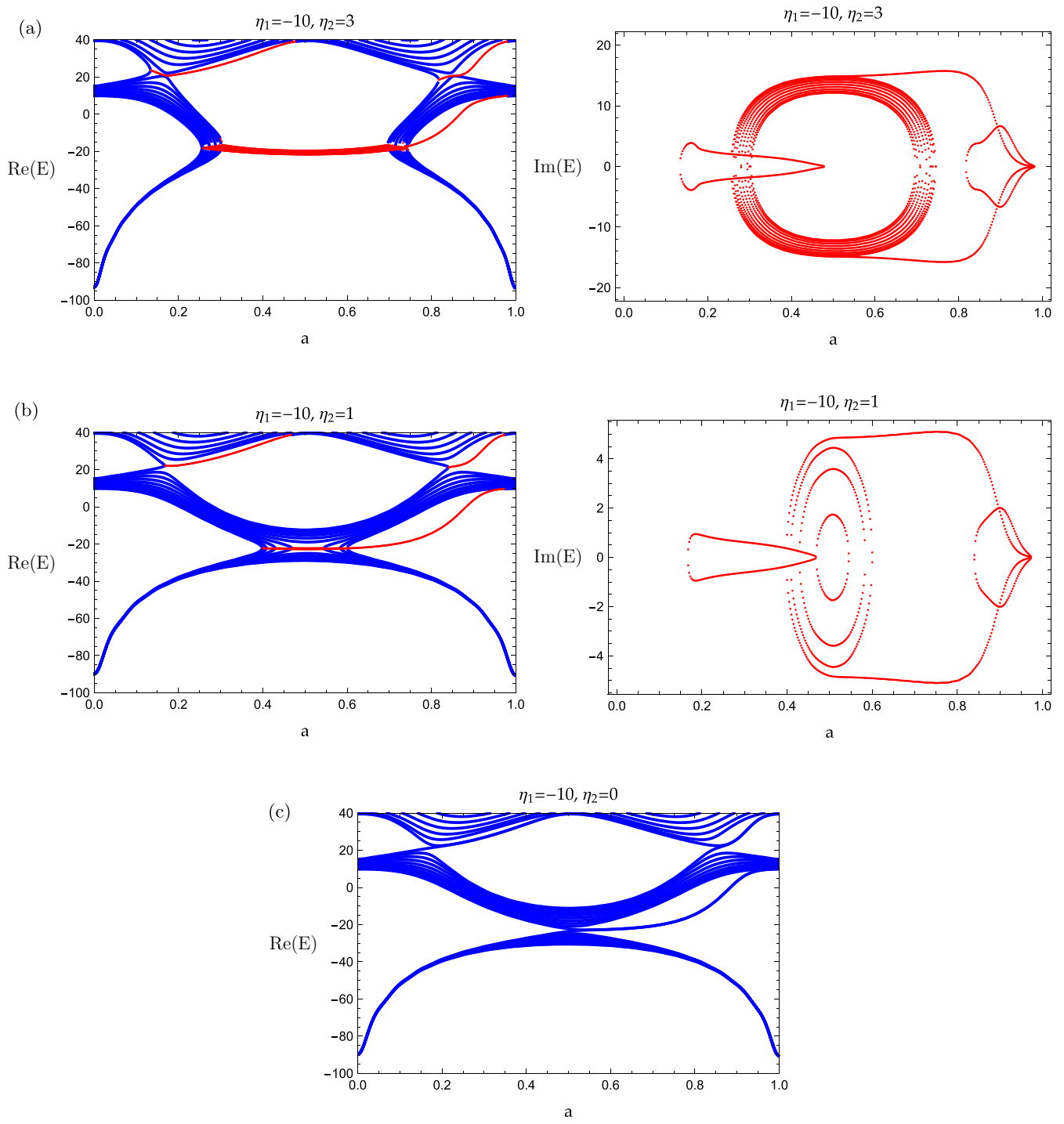

FIG. 3. The real and imaginary parts of energy spectrum as a function of the distance $a = 1 - b$ between two δ potentials z_1 and z_1^* for $\eta_1 = -10$ negative strength and varying η_2. The real energy solutions are plotted in blue, and the complex energy solutions are plotted in red. The number of cells is $M = 10$. (a) Real (left) and imaginary (right) parts of eigen-energy with $\eta_1 = -10$ and $\eta_2 = 3$. (b) Real (left) and imaginary (right) parts of eigen-energy with $\eta_1 = -10$ and $\eta_2 = 1$. (c) Real eigen-energy with $\eta_1 = -10$ and $\eta_2 = 0$.

these levels depend significantly on the matching conditions (or parameter a), and in a real crystal, due to the surface roughness, the states must be distributed over the gap (see, e.g., Ref. [36].

Now, let us first look at what happens to the band structure when $\eta_2 \neq 0$.

In order to further investigate the modification of the band structure, let us first complete the model by providing a more formal description when $\eta_1 = 0$ but $\eta_2 \neq 0$ (delta potentials have purely imaginary strengths). In this case, as can be seen from the characteristic determinant D_2 analysis [see Eq. (20)], the latter has no real roots for negative energy and $\mathcal{PT}$

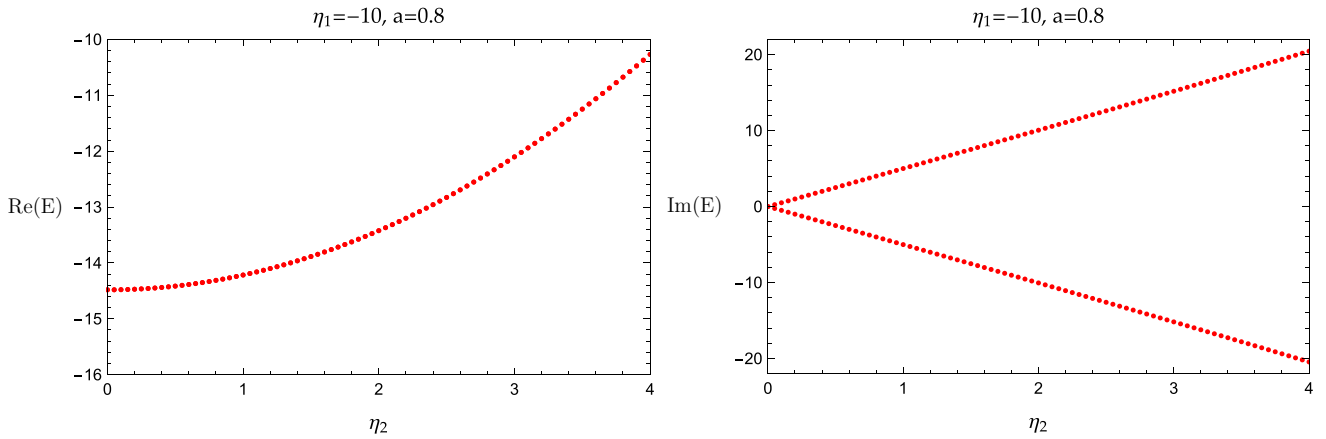

FIG. 4. The real and imaginary parts of the lowest edge state energy at $a = 0.8$ in Fig. 3 as a function of $\eta_2 \in [0, 4]$.

symmetry breaks down. For the general case with $\eta_1 \neq 0$, it is clear that the small values of η_2 ($\eta_2 \ll \eta_1$) do not change the general shape of the band structure, but they do change the values of the energy levels. As a result, one obtains the usual band structure for the complex potential as one would expect for a real periodic potential (22). However, as seen from Fig. 2(b) ($\eta_2 = 3$) and Fig. 2(a) ($\eta_2 = 5$), some states are already missing with increasing strength of the η_2. This applies mainly to the degenerate edge states that have separated from the upper band and move to lower band through the forbidden gap, accurately tracking the bulk bands trajectories [see panel $\eta_2 = 0$ in Fig. 2(c)]. To get more insight into the mathematical structures of the eigenvalues, we focus, for clarity and simplicity, on the case of model where $a = b$ (see, e.g., Refs. [2,37]). For this particular case, the dispersion relation (28) can be written in the form

$$\cos^2(\beta a) = \left(\cos(ka) + \frac{\eta_1}{2k}\sin(ka)\right)^2 + \frac{\eta_2^2}{4k^2}\sin^2(ka). \quad (29)$$

First, as it is clear from Eq. (29), $\beta a = \pi/2$ solution is not anymore available. Second, back to the case $a \neq b$, we can state that the disappearance of some states from the band structure and the further modification of the latter with increasing strength η_2 are associated mainly with the mentioned fact of the exclusion of some antiperiodic and even nonantiperiodic solutions from the dispersion Eq. (28) (see, e.g., Refs. [2,38]).

The physical meaning of the latter is completely transparent if we recall that up to a critical value η_{2cr} of the gain and loss parameter, η_2, eigenvalues are real [see Fig. 2(c)]. At the critical or exceptional value η_{2cr}, the eigenvalues and the eigenfunctions merge. Beyond the exceptional point, i.e., for $\eta_2 \geqslant \eta_{2cr}$, the system enters the region where some eigenvalues become complex, and complex conjugate pairs [see Figs. 2(a) and 2(b), right panels]. The latter means that the number of real eigenenergy has decreased. The theoretical description presented above is fully confirmed by numerical simulations as illustrated in Figs. 2(a) and 2(b). Indeed, as can be seen from the comparison of the imaginary parts of the numerical spectra of the self-energy (red lines) in Figs. 2(a) and 2(b), with the increasing of η_2 the number of complex levels increases. As a result, more states begin to move out from the given region, and further modification of band structures occurs [see, e.g., Figs. 2(a) and 2(b)].

The situation becomes even more interesting in the case of negative values of η_1, since for some values of η_{2cr} (see

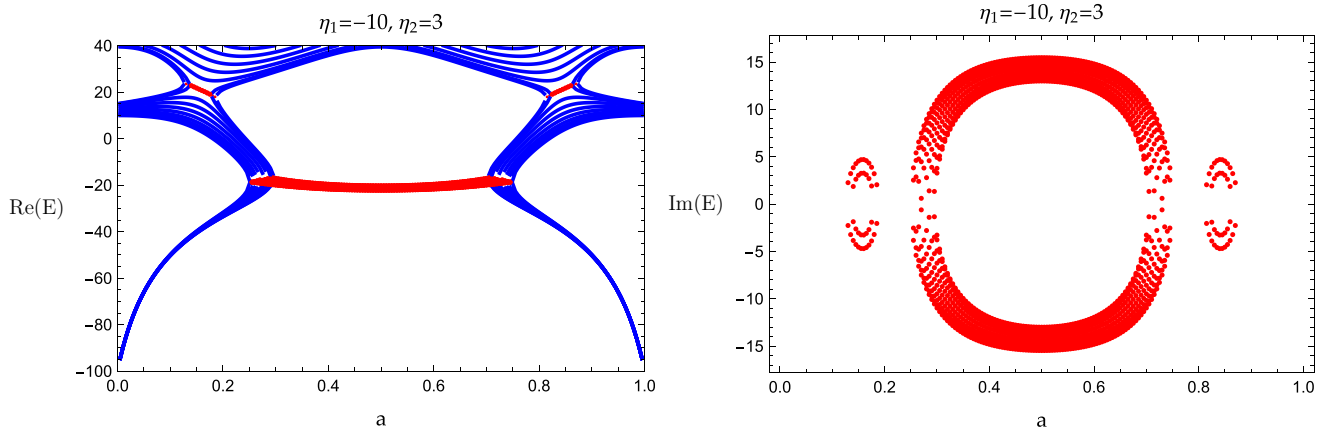

FIG. 5. The real and imaginary parts of energy spectrum for a periodic system at the limit of $M \to \infty$; energy spectra are determined by Eq. (28), where $\beta \in [0, \frac{2\pi}{d}]$ is quasimomentum of electron in a periodic system.

below) the topological states inherent in the case $\eta_2 = 0$ will be pushed out. The latter means that η_2 can break the underlying symmetry of the system, including chiral or time-reversal symmetry. To study in more detail the modification of the energy spectrum in Fig. 3, the band energy spectra of the finite chain for negative values of $\eta_1 = -10$ for different η_2 are shown. Recall that in the case of $\eta_1 < 0$ in transcendental equations (24) and (28), $k = \sqrt{-E}$ (we are in the range $E < 0$) must be replaced by $i\kappa$: as a consequence, trigonometric functions become hyperbolic. In Fig. 3(c) ($\eta_2 = 0$), one sees the existence of flat energy states in the middle of the band gap only when $a \geqslant 0.5$. This asymmetry reflects the fact that the number of scatterers in the system is even (see, e.g., Refs. [30,31,39]) and states are localized strongly over one side of the system. The effective mass of these states is very large due to the central position and, generally, they are insensitive to local perturbations, or in other words, any adiabatic deformation that respects certain symmetries of the system will not affect the existence of the symmetry-protected edge states (see, e.g., Refs. [30,31,35,39]). They are classified by topological invariants that remain unchanged under continuous deformations.

It turns out, however, that the situation is somewhat more complicated in $\mathcal{PT}$-symmetric systems, since including non-Hermitian parameter η_2 will eventually be crucial for getting insight into the physics of topological states (see, e.g., Ref. [40] and references therein). Esaki *et al.* [40] concluded that zero-energy modes are unstable and corresponding energy eigenvalues are not real. This conclusion is also confirmed by our analytical and numerical calculations for a one-dimensional $\mathcal{PT}$-symmetric superlattice built with quantum δ wells [Eq. (16) and Fig. 4]. However, for some special cases, such as the non-Hermitian generalized off-diagonal Aubry-Andre model [35], topological edge states with real spectrum have been discovered, provided η_2 is less than η_{2cr}. Note that these degenerate edge states are robust against small non-Hermitian perturbations.

Returning to the case of $\eta_2 \neq 0$, we note that a numerical analysis of expression (24) shows that as η_2 increases, the disappearance of some states from the band structure occurs even at small $\eta_2 \ll \eta_{cr}$ (not shown in Fig. 3). As η_2 increases further, disappearance of more and more levels takes place from the band structure [see red lines in Figs. 3(a) and 3(b)]. These lines represent the imaginary eigenvalues and are due to the fact that the spectrum is no longer real, unlike the $\eta_2 = 0$ case. Comparing the two real spectra of Figs. 3(b) and 3(c), we note that the real part of the spectrum is almost left unchanged except the lowest edge state energy that is pushed out from the given region [red line in Fig. 3(b)]. However, the band structure is drastically different for $\eta_2 = 3$ because more states begin to move out, and further modification of the band structure takes place. The red lines are very sensitive to the parameter η_2. We plot the real and imaginary parts of the lowest edge state energy at $a = 0.8$ as a function of η_2 in Fig. 4. As can be seen, actually, the complex conjugate eigenvalues appear whenever η_2 is different from zero (see the right panel in Fig. 4).

To determine η_{2cr} for the case of $a = b$, we solve Eqs. (24) and (28) simultaneously. After some algebra, we get

$$\eta_{2cr}^2 \leqslant \frac{2\kappa^2}{\sinh^2(\kappa a)}\left[1 + \cos\left(\frac{2\pi n}{2M+1}\right)\right], \quad n = 1, \ldots, 2M, \tag{30}$$

with the limit $a^2\eta_{2cr}^2 \leqslant 2[1 + \cos(\frac{2\pi n}{2M+1})]$ when $\kappa \to 0$. Inequality (30) is in a reasonable agreement with criterion (A3) in the sense that it is sensitive to the parameters characterizing the system, such as number of scatters M, distance between two successive delta potentials in unit cell, etc. (see below). As the number of cells M is increased, η_{2cr} demonstrates fast oscillating behavior due to $1 + \cos(\frac{2\pi n}{2M+1})$ function. The limiting condition of Eq. (30), when $M \to \infty$, reads $a\eta_{2cr} \leqslant 2$. With a further increase in $\eta \geqslant \eta_{2cr}$, we observe drastically different shape of the energy spectrum compared to the case $\eta_2 = 0$ [see Figs. 3(a) and 3(b)]. This means that $\mathcal{PT}$ symmetry breaks down and the eigenvalues of the bound states are complex numbers.

At the limit of $M \to \infty$, the $\mathcal{PT}$-symmetric system becomes periodic, and the energy spectrum is thus determined by Eq. (28), where $\beta \in [0, \frac{2\pi}{d}]$ denotes the quasimomentum of an electron in a periodic system. The topological edge states thus are eliminated in a periodic system; see, e.g., Fig. 5 compared with Fig. 3(a) for a finite system with hard wall boundary condition. An interesting observation is that the exceptional points could depend heavily on β, especially for negative energy bands (see, e.g., Fig. 5).

IV. SUMMARY AND OUTLOOK

The main result of this work is that we arrive at a closed-form expression for the energy spectrum of $\mathcal{PT}$-symmetric superlattice systems with two complex δ potentials in the elementary cell. It holds for both real and complex potentials, extending several well-known results in the literature, and helps to get even more insight into the mathematical structures of the eigenvalues. We analyzed in detail a diatomic crystal model, varying either the scatterer distances or the potential heights. It is shown that at a certain critical value of the imaginary part of the complex amplitude, the topological states may move out. This may happen at the $\mathcal{PT}$-symmetry breaking (exceptional) points.

ACKNOWLEDGMENTS

P.G. acknowledges support from the College of Arts and Sciences and Faculty Research Initiative Program, Dakota State University, Madison, SD. V.G., A.P.-G., and E.J. would like to thank UPCT for partial financial support through "Maria Zambrano ayudas para la recualificación del sistema universitario español 2021–2023" financed by Spanish Ministry of Universities with funds "Next Generation" of EU. This research was supported by the National Science Foundation under Grant No. NSF PHY-2418937 and in part by the National Science Foundation under Grant No. NSF PHY1748958.

DATA AVAILABILITY

No data were created or analyzed in this study.

APPENDIX: BROKEN AND UNBROKEN $\mathcal{PT}$-SYMMETRIC PHASES

It is known that η_2 represents non-Hermitian degree and describes the gain and loss rate that determines the existence of a real or complex energy spectrum in $\mathcal{PT}$-symmetric systems. One can show that the criterion for the eigenvalues of $\mathcal{PT}$-symmetric S-matrices to be unimodular is $r_L - r_R = \pm 2it$ (see, e.g., Refs. [12,37,41,42]). Depending on the physical context of the problem, a number of authors have estimated the critical value of η_{2cr} either based on the above criterion (see, e.g., Ref. [41]) or by diagonalizing the Hamiltonian and obtaining the energy spectrum numerically (see, e.g., Ref. [9]), or by relating the problem to an solvable effective two-state Hamiltonian problem that holds only in the thermodynamic limit (see, e.g., Refs. [23,43]). At this limit, near the critical point, all microscopic details of the system will eventually become irrelevant, contrary to what would be expected from the finite system. Regarding the latter, some analytical/numerical results for the critical frequency at which the symmetry breaking phase occurs in a complex index dielectric slab or in an arbitrary one-dimensional finite periodic scatterer or predicting the $\mathcal{PT}$ symmetry breaking point for edge states in finite lattices are published in Refs. [23,41,42]. Based on a tight-biding model and assuming $\eta_1 = 0$, it was shown that the transition from weak non-Hermiticity to the regime of strong non-Hermiticity is controlled by the ratio $\frac{\eta_2}{2t_h}$ (t_h is the amplitude of the jump between two sites and a gain/loss pair controlled by the $\mathcal{PT}$ η_2 parameter) (see, e.g., Refs. [11,44,45]). The behavior of the transmission probability is strongly non-Hermitian in the regime of weak non-Hermiticity with divergent peaks when $\frac{\eta_2}{2t_h} < 1$ and is almost Hermitian in the regime of strong non-Hermiticity, $\frac{\eta_2}{2t_h} > 1$. For a simplified continuum model consisting of two complex delta potentials, it was found that divergent peaks of the transmission and reflection coefficients appear in the range $\frac{\eta_2}{2k} < 1$ (see, e.g., Refs. [9,15,16,44]).

In what follows, we will rewrite the above criterion $r_L - r_R = \pm 2it$ for broken symmetry phase/$\mathcal{PT}$-symmetric phase in a slightly different, but completely equivalent form. This consists of mapping the mentioned criterion onto a one-dimensional partial differential equation, leaving only one parameter t. We will see that the result obtained with the new criterion is consistent with continuum results obtained elsewhere using single-particle scattering from an absorbing delta potential (see, e.g., Refs. [42,43,46]).

To this end, we focus on the case $Z_1 = Z_N^* = \eta_1 + i\eta_2$ and note that using expressions (8) and (9) for r_L and r_R the criterion $r_L - r_R = \pm 2it$ can be rewritten in equivalent form

$$\frac{\partial}{\partial Z_N}\frac{1}{t}\bigg|_{cr} - \frac{\partial}{\partial Z_1}\frac{1}{t}\bigg|_{cr} = \pm\frac{1}{k}. \tag{A1}$$

Using the chain rule and rewriting the above equation in terms of partial derivatives with respect to η_1 and η_2, we arrived at

$$i\frac{\partial}{\partial \eta_2}\frac{1}{t}\bigg|_{cr} = \pm\frac{1}{k}. \tag{A2}$$

Integrating both sides of the equation and assuming that an arbitrary function representing the constant of integration with respect to η_2 is not zero, say $\frac{1}{t_0}$, the solution can be presented in the form

$$\frac{1}{t}\bigg|_{cr} = \mp\frac{i\eta_{2cr}}{k} + \frac{1}{t_0}. \tag{A3}$$

Criterion (A3) for $1/t_{cr}$ depends solely on η_{2cr}/k (first term) and on the form of the 1D shape of the potential (second term). The particular solution, when $\frac{1}{t_0}$ is zero, nicely reproduces the transmission amplitude as a function of the strength of the imaginary part of complex δ function at an exceptional point, i.e., around $\eta_2 \approx k$. This also allows us to understand, at least at a qualitative level, why diverging peaks of transmission and reflection coefficients appear in the range $\frac{\eta_2}{2k} < 1$ (see, e.g., Refs. [15,16,44]). It is easy to get convinced that if the constant $\frac{1}{t_0}$ of integration over η_2 is not equal to zero, then the explicit value of η_{cr} is generally very complex and depends on the shape of the potential.

[1] C. M. Bender and S. Boettcher, Real spectra in non-Hermitian Hamiltonians having PT symmetry, Phys. Rev. Lett. **80**, 5243 (1998).

[2] H. F. Jones, The energy spectrum of complex periodic potentials of the Kronig–Penney type, Phys. Lett. A **262**, 242 (1999).

[3] I. Crassee, J. Levallois, A. L. Walter, M. Ostler, A. Bostwick, E. Rotenberg, T. Seyller, D. van der Marel, and A. B. Kuzmenko, Giant Faraday rotation in single- and multilayer graphene, Nat. Phys. **7**, 48 (2011).

[4] A. Guo, G. J. Salamo, D. Duchesne, R. Morandotti, M. Volatier-Ravat, V. Aimez, G. A. Siviloglou, and D. N. Christodoulides, Observation of $\mathcal{PT}$-symmetry breaking in complex optical potentials, Phys. Rev. Lett. **103**, 093902 (2009).

[5] A. A. Zyablovsky, A. P. Vinogradov, A. A. Pukhov, A. V. Dorofeenko, and A. A. Lisyansky, PT-symmetry in optics, Phys. Usp. **57**, 1063 (2014).

[6] K. G. Makris, R. El-Ganainy, D. N. Christodoulides, and Z. H. Musslimani, Beam dynamics in $\mathcal{PT}$ symmetric optical lattices, Phys. Rev. Lett. **100**, 103904 (2008).

[7] R. K. Dani, H. Wang, S. H. Bossmann, G. Wysin, and V. Chikan, Faraday rotation enhancement of gold coated Fe_2O_3 nanoparticles: Comparison of experiment and theory, J. Chem. Phys. **135**, 224502 (2011).

[8] R. El-Ganainy, K. G. Makris, M. Khajavikhan, Z. H. Musslimani, S. Rotter, and D. N. Christodoulides, Non-Hermitian physics and PT symmetry, Nat. Phys. **14**, 11 (2018).

[9] P. C. Burke, J. Wiersig, and M. Haque, Non-Hermitian scattering on a tight-binding lattice, Phys. Rev. A **102**, 012212 (2020).

[10] P.-P. Huang, J. He, J.-R. Li, H.-N. Wu, L.-L. Zhang, Z. Jin, and W.-J. Gong, Transmission through a one-dimensional photonic lattice modulated by the side-coupled PT-symmetric non-Hermitian Su–Schrieffer–Heeger chain, J. Opt. Soc. Am. B **38**, 1331 (2021).

[11] J. Zheng, X. Yang, D. Deng, and H. Liu, Singular properties generated by finite periodic PT-symmetric

optical waveguide network, Opt. Express **27**, 1538 (2019).
[12] L. Ge, Y. D. Chong, and A. D. Stone, Conservation relations and anisotropic transmission resonances in one-dimensional $\mathcal{PT}$-symmetric photonic heterostructures, Phys. Rev. A **85**, 023802 (2012).
[13] A. Basiri, I. Vitebskiy, and T. Kottos, Light scattering in pseudopassive media with uniformly balanced gain and loss, Phys. Rev. A **91**, 063843 (2015).
[14] P. Guo and V. Gasparian, Friedel formula and Krein's theorem in complex potential scattering theory, Phys. Rev. Res. **4**, 023083 (2022).
[15] P. Guo, V. Gasparian, E. Jódar, and C. Wisehart, Tunneling time in $\mathcal{PT}$-symmetric systems, Phys. Rev. A **107**, 032210 (2023).
[16] V. Gasparian, P. Guo, A. Pérez-Garrido, and E. Jódar, Tunneling time and Faraday/Kerr effects in $\mathcal{PT}$-symmetric systems, Europhys. Lett. **143**, 66001 (2023).
[17] P. Guo, V. Gasparian, A. Pérez-Garrido, and E. Jódar, Tunneling time in coupled-channel systems, Phys. Rev. Res. **6**, 043032 (2024).
[18] V. Gasparian, P. Guo, and E. Jódar, Anomalous Faraday effect in a PT-symmetric dielectric slab, Phys. Lett. A **453**, 128473 (2022).
[19] A. Perez-Garrido, P. Guo, V. Gasparian, and E. Jódar, Polar magneto-optic Kerr and Faraday effects in finite periodic $\mathcal{PT}$-symmetric systems, Phys. Rev. A **107**, 053504 (2023).
[20] V. M. Gasparian, B. L. Altshuler, A. G. Aronov, and Z. A. Kasamanian, Resistance of one-dimensional chains in Kronig-Penny-like models, Phys. Lett. A **132**, 201 (1988).
[21] V. Gasparian and M. Pollak, Büttiker-Landauer characteristic barrier-interaction times for one-dimensional random layered systems, Phys. Rev. B **47**, 2038 (1993).
[22] V. Gasparian, U. Gummich, E. Jódar, J. Ruiz, and M. Ortuño, Tunneling and dwell time for one-dimensional generalized Kronig-Penney model, Phys. B: Condens. Matter **233**, 72 (1997).
[23] A. F. Tzortzakakis, A. Katsaris, N. E. Palaiodimopoulos, P. A. Kalozoumis, G. Theocharis, F. K. Diakonos, and D. Petrosyan, Topological edge states of the $\mathcal{PT}$-symmetric Su-Schrieffer-Heeger model: An effective two-state description, Phys. Rev. A **106**, 023513 (2022).
[24] L. Jin, Topological phases and edge states in a non-Hermitian trimerized optical lattice, Phys. Rev. A **96**, 032103 (2017).
[25] Z. A. Kasamanian, On the theory of impurity levels, Sov. Phys. JETP **34**, 648 (1972) [Zh. Eksp. Teor. Fiz. **61**, 1215 (1971)].
[26] E. N. Economou, *Green's Functions in Quantum Physics*, *Springer Series in Solid-State Sciences* (Springer, Berlin, 2006).
[27] Z. A. Kasamanyan, Local density of states in a model variable-band semiconductor, Sov. Phys. J. **24**, 525 (1981).
[28] V. Gasparian, B. Altshuler, and M. Ortuño, Charge pumping in one-dimensional Kronig-Penney models, Phys. Rev. B **72**, 195309 (2005).
[29] A. G. Aronov, V. M. Gasparian, and U. Gummich, Transmission of waves through one-dimensional random layered systems, J. Phys.: Condens. Matter **3**, 3023 (1991).
[30] T. B. Smith and A. Principi, "A bipartite Kronig–Penney model with Dirac-delta potential scatterers, J. Phys.: Condens. Matter **32**, 055502 (2020).
[31] I. Reshodko, A. Benseny, J. Romhányi, and T. Busch, Topological states in the Kronig–Penney model with arbitrary scattering potentials, New J. Phys. **21**, 013010 (2019).
[32] M. Belloni and R. W. Robinett, The infinite well and Dirac delta function potentials as pedagogical, mathematical and physical models in quantum mechanics, Phys. Rep. **540**, 25 (2014).
[33] P. Pedram and M. Vahabi, Exact solutions of a particle in a box with a delta function potential: The factorization method, Am. J. Phys. **78**, 839 (2010).
[34] C. De Lange and T. Janssen, Modulated Kronig-Penney model in superspace, Physica A **127**, 125 (1984).
[35] C. Yuce, Topological phase in a non-Hermitian PT symmetric system, Phys. Lett. A **379**, 1213 (2015).
[36] B. L. Oksengendler, V. N. Nikiforov, and S. E. Maksimov, Tamm states of fractal surfaces, Dokl. Phys. **62**, 281 (2017).
[37] Z. Ahmed, J. A. Nathan, and D. Ghosh, Transparency of the complex PT-symmetric potentials for coherent injection, Phys. Lett. A **380**, 562 (2016).
[38] Z. Ahmed, Energy band structure due to a complex, periodic, PT-invariant potential, Phys. Lett. A **286**, 231 (2001).
[39] L. Peyruchat, R. H. Rodriguez, J.-L. Smirr, R. Leone, and Ç. Ö. Girit, Spectral signatures of nontrivial topology in a superconducting circuit, Phys. Rev. X **14**, 041041 (2024).
[40] K. Esaki, M. Sato, K. Hasebe, and M. Kohmoto, Edge states and topological phases in non-Hermitian systems, Phys. Rev. B **84**, 205128 (2011).
[41] Y. D. Chong, L. Ge, and A. D. Stone, $\mathcal{PT}$-symmetry breaking and laser-absorber modes in optical scattering systems, Phys. Rev. Lett. **106**, 093902 (2011).
[42] V. Achilleos, Y. Aurégan, and V. Pagneux, Scattering by finite periodic $\mathcal{PT}$-symmetric structures, Phys. Rev. Lett. **119**, 243904 (2017).
[43] S. Garmon, M. Gianfreda, and N. Hatano, Bound states, scattering states, and resonant states in $\mathcal{PT}$-symmetric open quantum systems, Phys. Rev. A **92**, 022125 (2015).
[44] K. Shobe, K. Kuramoto, K.-I. Imura, and N. Hatano, Non-Hermitian Fabry-Pérot resonances in a PT-symmetric system, Phys. Rev. Res. **3**, 013223 (2021).
[45] L. Jin and Z. Song, Solutions of $\mathcal{PT}$-symmetric tight-binding chain and its equivalent Hermitian counterpart, Phys. Rev. A **80**, 052107 (2009).
[46] J. G. Muga, J. P. Palao, B. Navarro, and I. L. Egusquiza, Complex absorbing potentials, Phys. Rep. **395**, 357 (2004).